CONDENSED MATTER

Correlation Between Magnetic and Electric Properties in the Series of $Co_xZn_{1-x}Fe_2O_4$ Nanoparticles

D. Petrov[a,*], I. Edelman[a,b], A. Thakur[c], P. Thakur[c], A. Sukhachev[a], and S. Ovchinnikov[a,b]

[a] Kirensky Institute of Physics, Federal Research Center KSC, Siberian Branch, Russian Academy of Sciences, Krasnoyarsk, 660036 Russia

[b] Siberian Federal University, Krasnoyarsk, 660041 Russia

[c] Amity University Haryana, Gurugram, Haryana, 122413 India

*e-mail: irbiz@iph.krasn.ru

Received March 30, 2023; revised April 11, 2023; accepted April 11, 2023

Magnetization dependences of $Co_xZn_{1-x}Fe_2O_4$ nanoparticles ($x = 0, 0.1, 0.2, 0.3, 0.4, 0.5$) synthesized with the citrate precursor technique on an external magnetic field and temperature are presented. Ferrimagnetic order in nanoparticles with $x \geq 0.2$ appeared at temperatures, T, exceeding room temperature, and in nanoparticles with $x = 0$ and 0.1 at T near 100 K. The saturation magnetization, M_s, remnant magnetization, M_r, and the coercive force, H_c, increase with x increase and the temperature decrease. M_s reached very high value: M_s of NPs with $x = 0.5$ equals to 106.6 emu/g at 100 K while, according to the literature data, M_s of stoichiometric bulk Co ferrite equals to 90 emu/g at 4.2 K. Correlations between concentration dependences of magnetic and electric properties has been revealed and explained qualitatively.

Mixed spinel ferrites ($Co_xZn_{1-x}Fe_2O_4$) attract great attention due to their unique properties such as high specific electrical resistivity and low eddy current losses [1−5], high saturation magnetization and Curie temperature [6], thermodynamic stability, corrosion resistance, high mechanical hardness, strong adsorption capacity. Nanoparticles (NPs) with different Co and Zn relative concentrations have an impressive range of applications: active components of ferromagnetic (FM) fluids, permanent magnets, computer components, systems for targeted drug delivery, resonance imaging, and many others (see, e.g., [7]). The extreme members $ZnFe_2O_4$ and $CoFe_2O_4$ have the same crystalline spinel structure of the *Fd*-3*m* space group but differ in the cations distribution between crystalline positions. $ZnFe_2O_4$ is the normal spinel where divalent Zn^{2+} ions occupy tetrahedral positions and trivalent Fe^{3+} ions are situated in octahedral positions. In the inverse spinel $CoFe_2O_4$, a half of Fe^{3+} ions occupy tetrahedral and other half of these ions, octahedral positions while Co^{2+} ions prefer octahedral positions. According to these cation distributions, $ZnFe_2O_4$ is characterized by the antiferromagnetic (AFM) order with the low Neel temperature, $T_N = 10$ K, and $CoFe_2O_4$ is ferrimagnet with high Curie temperature, $T_c = 793$ K, and the room temperature saturation magnetization $M_s = 66.3$ emu/g [7]. However, devia-

tions from this ideal distribution are observed frequently in the case of NPs due to the low particles dimension, surface effects, high concentration of surface defects [8]. The degree of inversion can be presented with the formulae $(Zn_{1-\delta}Fe_\delta) [Zn_\delta Fe_{2-\delta}] O_4$, where parentheses and square brackets refer to tetrahedral (A) and octahedral (B) positions, respectively. Several authors synthesized partially inverted Zn-ferrite NPs which were ferrimagnetic at room temperature with the saturation magnetization varying from 10 to 88 emu/g in dependence on the synthesis technique. A wide variety of cation distributions over the crystal positions and magnetic properties were observed by several authors for the case of mixed spinels $Zn_{1-x}Co_xFe_3O_4$ NPs (e.g., [9−13]). Thus, technological conditions had an extremely strong effects in the properties of the synthesized NPs which emphasizes the need to study thoroughly magnetic characteristics of obtained samples in each case.

Recently, a series of $Co_xZn_{1-x}Fe_2O_4$ NPs with x varying from 0.0 to 0.5 were prepared by citrate precursor technique which demonstrated a remarkable electric resistivity and improved dielectric properties [14]. The value of the dielectric loss tangent varied in the range 0.003−0.052 at 1 MHz for different Co concentrations, and the samples were found to be very good insulators. The study of magnetic properties of this NPs system undertaken in the present work seems
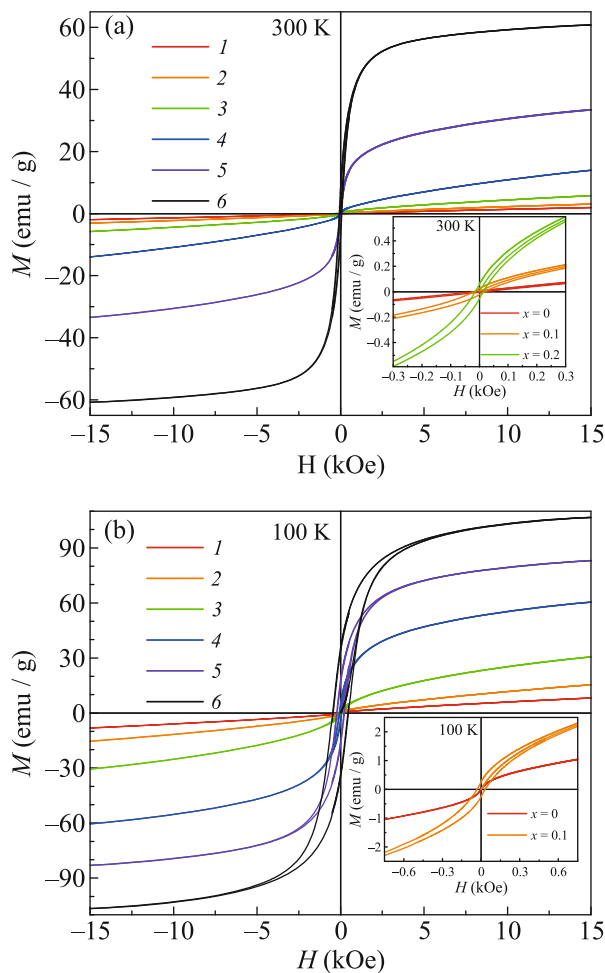
Fig. 1. (Color online) Field dependences of magnetization of samples 1−6 measured at T = (a) 300 and (b) 100 K. Insets: magnetization curves of samples (a) 1−3 and (b) 1 and 2.

to be of importance from the point of view of the relationship between the electronic and magnetic subsystems and the NPs applications.

Technology of the synthesis of the $Co_xZn_{1-x}Fe_2O_4$ NPs with (x = 0, 0.1, 0.2, 0.3, 0.4, 0.5 (samples 1−6, respectively)) was described in details in [14]. X-ray diffraction study revealed the spinel phase cubic structure of the Fd-$3m$ space group. The average crystallite size of the samples was found to be in the range of 28−36 nm. The lattice constant decreased from 8.443 to 8.403 Å with an increase in cobalt concentration which was associated with the smaller Co^{2+} ion radius (0.72 Å) comparing to the Zn^{2+} ion radius (0.74 Å). Magnetization dependences on an external magnetic field and temperature were studied with the vibrating sample magnetometer Lake Shore 8604 in magnetic field up to 15 kOe at temperatures from 90 to 350 K.

Magnetization (M) curves of samples 1−6 versus applied magnetic field (H) at 300 and 100 K are pre-

sented in Figs. 1a and 1b, respectively. Only the sample 1 with x = 0 demonstrates a pure paramagnetic behavior at room temperature. Even for the sample 2 with x = 0.1, the room temperature magnetization curve deviates from the linear dependence on H characteristic of a paramagnetic substance, and in the case of sample 3 with x = 0.2, a very narrow hysteresis loop is clearly visible.

At the same time, with an increase in the magnetic field, the magnetization of these three samples increases linearly in the field, differing significantly from the course of the magnetization curves of samples 4−6. It can be assumed that some of the NPs in samples 2 and 3 are in the superparamagnetic state at room temperature, while most of the particles in those samples are paramagnetic. In the case of samples 4−6 the shape of the magnetization curves indicates the superparamagnetic state of the main part of NPs, and the presence of hysteresis may mean that some of the superparamagnetic NPs are blocked at room temperature. At that, a sharp magnetization increase is observed at the transition from sample 3 to sample 4 which can be interpreted as a transition from a heterogeneous magnetic state of the entire ensemble of NPs, in which paramagnetic and superparamagnetic NPs coexist, to the superparamagnetic state of most NPs. The similar picture was observed in [12, 13, 15, 16].

As the temperature decreases to 100 K, the superparamagnetic component appears in sample 1, which does not contain Co. This follows from a change in the shape of the magnetization curve: a characteristic s-shaped bend appears near zero. An appearance of the magnetic moment in the $ZnFe_2O_4$ NPs was observed earlier (e.g., [9]), but not always. For example, magnetic ordering was not observed up to 50 K in Zn spinel NPs obtained with co-precipitation method [2, 12]. For all other samples, upon cooling, a strong increase in the magnetization is observed. Remanence M_r and coercivity H_c also increase when cooling but to varying degrees.

The temperature dependences of the magnetization (Fig. 2) of samples 1−5 recorded in a magnetic field of 5 kOe are similar to the FC curves for $Co_xZn_{1-x}Fe_2O_4$ NPs synthesized with the precursor combustion method shown in [12]. Several mechanisms are responsible for the increase in the magnetization of NPs with decreasing temperature. Among them, the increase in the magnetic moment itself of each NPs obeys the Curie law for paramagnets or the Langevin's law for magnetically ordered media, as well as the alignment of magnetic moments in the direction of the applied magnetic field. The shape of the temperature dependence curves confirms the conclusion made during the interpretation of the magnetization curves about the concentration transition from the predominantly paramagnetic to the superparamagnetic state of NPs between Co concentrations x = 0.2 and 0.3.
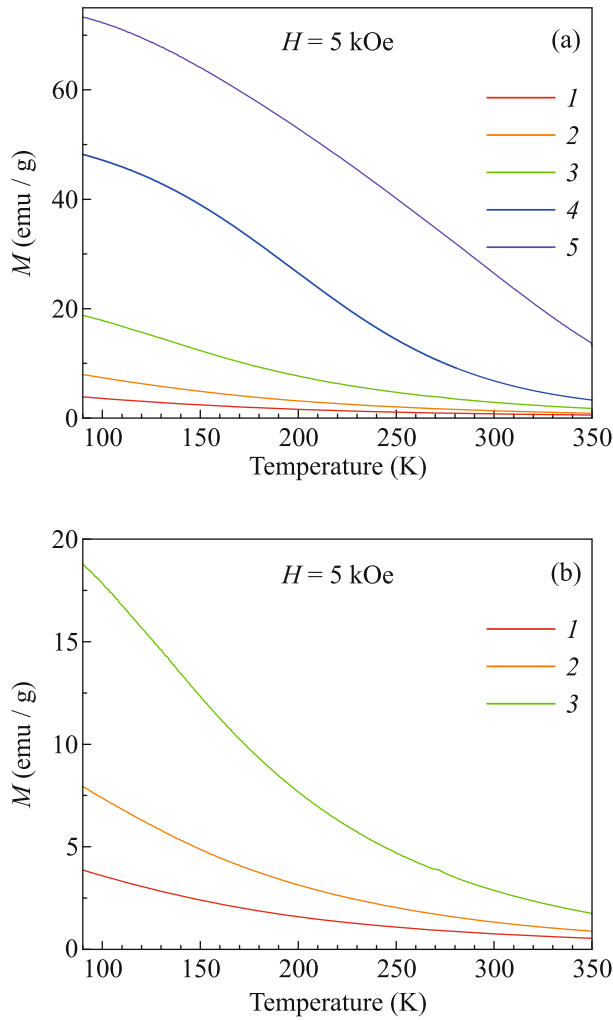
Fig. 2. (Color online) Magnetization temperature dependences for (a) samples 1−5, curves *1−5* with $x = 0−0.4$, respectively, and (b) the same for samples with $x = 0−0.2$, curves *1−3*, in a magnetic field of 5 kOe.

Fig. 3. (Color online) Concentration dependences of H_c, M_r, and the electric current at a voltage of 3 V from [14].

It is interesting to note some correlations between the concentration dependences of the magnetic and electric properties of the studied samples. In Fig. 3, the concentration dependences of the coercivity and remnant magnetization are shown in comparison with the concentration dependence of the electric current passing through the sample at a voltage of 3 V, obtained from the current-voltage characteristics. Co−Zn ferrite NPs were pressed into pellets to carry out electric properties investigation.

An increase of the electric current with the Co concentration increase shown in Fig. 3 means decreasing resistivity. In the mixture of $ZnFe_2O_4$ and $CoFe_2O_4$ decreasing resistivity results from a smaller resistivity of $CoFe_2O_4$ vs. $ZnFe_2O_4$. To understand why the resistivity of Co ferrites may be smaller, we may consider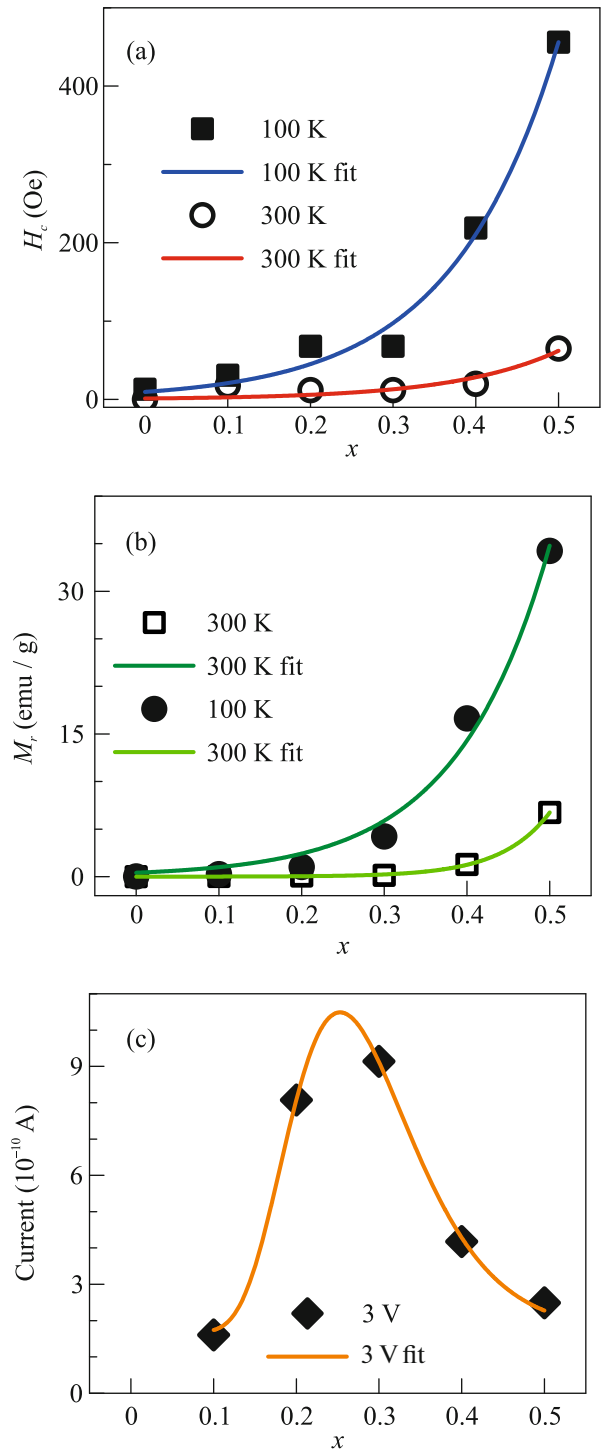 the electronic structure calculations within the density function theory (DFT). Such calculation for $CoFe_2O_4$ has been done by [17]. In this paper, the generalized gradient approximation with PBE potential and Hubbard U correction had been used to calculate the electronic structure for different set of exchange parame-

ters: MS1 configuration with FM Co−Co and Fe−Fe and AFM Co−Fe exchange, MS2 with all FM exchanges, MS3 with AFM Co−Co and FM Fe−Fe interactions, and MS4 with FM Co−Co and AFM Fe−Fe. While the insulator gap in the density of states (DOS) had been obtained for MS1, MS2, and MS3 configurations, the MS4 state is almost conductor with a band gap close to zero.

In the nanocrystalline samples discussed in this paper there is a mixture of Fe, Co, and Zn cations in different sublattices, that may be considered as the mixture of all four possible configurations. If this mixture is random, the 25% of the conducting phase will results in the macroscopic conductivity of the whole sample according to the percolation theory ideas. In 3D lattices with a random mixture of insulating and conducting phases the macroscopic conductivity occurs above the percolation threshold $x_c = 0.16$ [18].

Correlation of magnetic and electrical properties in Fig. 3 as well as concentration dependence of the dc resistivity on the Co concentration in Fig. 12 of the paper [14] can be explained within the percolation theory. The minimum resistivity in the $Co_xZn_{1-x}Fe_2O_4$ in Fig. 12 in [14] is found for $x = 0.2$ and 0.3, just above the percolation threshold.

CONFLICT OF INTEREST

The authors declare that they have no conflicts of interest.

REFERENCES

1. M. A. Mousa, A. M Summan, M. A. Ahmed, and A. M. Badawy, J. Mater. Sci. **24**, 2478 (1989).

2. T. Slatineanu, A. R. Iordan, V. Oancea, M. N. Palamaru, I. Dumitru, C. P. Constantin, and O. F. Caltun, J. Mater. Sci. Eng. B **178**, 1040 (2013).

3. A. S. Kamzin, I. M. Obaidat, V. G. Semenov, V. Narayanaswamy, I. A. Al-Omari, B. Issa, and I. V. Buryanenko, Phys. Solid State **6**, 714 (2022).

4. A. S. Kamzin, I. M. Obaidat, V. G. Semenov, V. Narayanaswamy, I. A. Al-Omari, B. Issa, and I. V. Buryanenko, Phys. Solid State **65**, 482 (2022).

5. Yu. S. Gaiduk, E. V. Korobko, K. A. Shevtsova, D. A. Kotikov, I. A. Svito, A. E. Usenko, D. V. Ivashenko, A. Fahmy, and V. V. Pankov, Phys. Solid State **22**, 28 (2022).

6. J. Smit and H. P. Wijn, *Ferrites. Physical Properties of Ferrimagnetic Oxides in Relation to their Technical Applications* (Philips' Techn. Libr., Eindhoven, 1959).

7. R. Sagayaraj, S. Aravazhi, and G. Chandrasekaran, Int. Nano Lett. **11**, 307 (2021).

8. C. Yao, Q. Zeng, G. F. Goya, T. Torres, J. Liu, H. Wu, M. Ge, Y. Zeng, Y. Wang, and J. Z. Jiang, J. Phys. Chem. C **111**, 12274 (2007).

9. R. Ramadan, M. K. Ahmed, and V. Uskokovic, J. Alloys Compd. **856**, 157013 (2021).

10. F. Gozuak, Y. Koseoglu, A. Baykal, and H. Kavasa, J. Magn. Magn. Mater. **321**, 2170 (2009).

11. S. G. C. Fonseca, L. S. Neiva, M. A. R. Bonifácio, P. R. C. dos Santos, U. C. Silva, and J. B. L. de Oliveira, Mater. Res. **21**, 20170861 (2018).

12. P. A. Asogekar, S. K. Gaonkar, A. Kumar, and V. M. S. Verenkar, Mater. Res. Bull. **141**, 111330 (2021).

13. T. Tatarchuk, M. Bououdina, W. Macyk, O. Shyichuk, N. Paliychuk, I. Yaremiy, B. Al-Najar, and M. Pacia, Nanoscale Res. Lett. **12**, 141 (2017).

14. D. Chahar, S. Taneja, P. Thakur, and A. Thakur, J. Alloys Compd. **843**, 155681 (2020).

15. G. Fan, J. Tong, and F. Li, Ind. Eng. Chem. Res. **51**, 13639 (2012).

16. W. S. Mohamed, M. Alzaid, M. S. M. Abdelbaky, Z. Amghouz, S. García-Granda, and A. M. Abu-Dief, Nanomaterials **9**, 1602 (2019).

17. I. P. Duru, Phys. B (Amsterdam, Neth.) **627**, 413548 (2022).

18. J. M. Ziman, *Models of Disorder* (Cambridge Univ. Press, New York, 1979).